

One-armed spiral structure of accretion discs induced by a phase-dependent mass transfer in Be/X-ray binaries

Kimitake Hayasaki^{1,2*} and Atsuo T. Okazaki³

¹*Department of Applied Physics, Graduate School of Engineering, Hokkaido University, Kitaku N13W8, Sapporo 060-8628, Japan.*

²*Centre for Astrophysics and Supercomputing, Swinburne University of Technology, Hawthorn Victoria 3122 Australia.*

³*Faculty of Engineering, Hokkai-Gakuen University, Toyohira-ku, Sapporo 062-8605, Japan.*

Received ...; accepted ...

ABSTRACT

We study non-axisymmetric structure of accretion discs in Be/X-ray binaries, performing three dimensional Smoothed Particle Hydrodynamics simulations for a coplanar system with a short period and a moderate eccentricity. We find that ram pressure due to the phase-dependent mass transfer from the Be-star disc excites a one-armed, trailing spiral structure in the accretion disc around the neutron star. The spiral wave is transient; it is excited around the periastron passage, when the material is transferred from the Be disc, and is gradually damped afterwards. The disc changes its morphology from circular to eccentric with the development of the spiral wave, and then from eccentric to circular with the decay of the wave during one orbital period. It turns out that the inward propagation of the spiral wave significantly enhances the mass-accretion rate onto the neutron star. Thus, the detection of an X-ray luminosity peak corresponding to the peak in enhanced mass-accretion rate provides circumstantial evidence that an accretion disc is present in Be/X-ray binaries.

Key words: accretion, accretion discs – hydrodynamics – methods: numerical – binaries: general – stars: emission-line, Be – X-rays: binaries

1 INTRODUCTION

About two-thirds of high-mass X-ray binaries have been identified as Be/X-ray binaries. These systems generally consist of a neutron star and a Be star with a cool ($\sim 10^4 K$) equatorial disc, which is geometrically thin and nearly Keplerian. Be/X-ray binaries are distributed over a wide range of orbital periods ($10 \text{ d} \lesssim P_{\text{orb}} \lesssim 300 \text{ d}$) and eccentricities ($e \lesssim 0.9$).

Most Be/X-ray binaries show only transient activity in X-ray emission and are termed Be/X-ray transients. Be/X-ray transients show periodic (Type I) outbursts, which are separated by the orbital period and have luminosity $L_X = 10^{36-37} \text{ erg s}^{-1}$, and giant (Type II) outbursts of $L_X \gtrsim 10^{37} \text{ erg s}^{-1}$ with no orbital modulation. These outbursts have features that strongly suggest the presence of an accretion disc around the neutron star.

Recently, Hayasaki & Okazaki (2004, hereafter paper I) studied the accretion flow around the neutron star in a Be/X-ray binary with a short period ($P_{\text{orb}} = 24.3 \text{ d}$) and a moderate eccentricity ($e = 0.34$), using a three dimensional Smoothed Particle Hydrodynamics (SPH) code. They

found that a time-dependent accretion disc is formed around the neutron star. They also discussed the evolution of the azimuthally-averaged structure of the disc, although the disc is significantly eccentric in spite of the nearly Keplerian rotation. The non-axisymmetric structure seen in the disc is considered to result from a phase-dependent mass transfer from the Be disc.

Tosa (1994) showed numerically that ram pressure due to an intergalactic gas excites the one-armed spiral structure in the non-selfgravitating, galactic V -constant disc. Then Kato & Tosa (1994) showed analytically that the excitation of the one-armed mode is caused by the same resonant instability mechanism as the tidally induced eccentric instability which explains the superhump phenomena in dwarf novae systems (Hirose & Osaki 1989, Lubow 1991). In the context of accretion disc theory, Lubow (1994) investigated the effect of time varying mass-transfer on the eccentricity of an accretion discs in a circular binary. However, it has never been explicitly studied how phase-dependent mass transfer affects the eccentricity of an accretion disc in an eccentric binary.

In this *letter*, we study the non-axisymmetric structure of the accretion disc around the neutron star in Be/X-ray binaries. In Section 2, the development of the one-armed

* E-mail: hayasaki@topology.coe.hokudai.ac.jp

spiral structure is demonstrated with 3D SPH simulations. The strength of several modes excited in the disc, the orbital modulation of the disc radius and the phase dependence of the mass-accretion rate are also analyzed in this section. Our conclusions are presented in Section 3.

2 RAM-PRESSURE-DEFORMED ACCRETION DISCS

In this section, we show that ram pressure due to the material transferred from the Be disc around periastron temporarily excites the one-armed spiral wave in the accretion disc around the neutron star in Be/X-ray binaries.

Our simulations were performed using the same 3D SPH code as in paper I, which was based on a version originally developed by Benz (Benz 1990; Benz et al. 1990) and later by Bate, Bonnell & Price (1995). In order to investigate the effect of ram pressure on the accretion disc, we compare results from model 1 in paper I (hereafter, model A) with those from a simulation (hereafter, model B) in which the mass transfer from the Be disc is artificially stopped for one orbital period. Except for this difference, the two simulations have the same model parameters: The orbital period P_{orb} is 24.3 d, the eccentricity e is 0.34, and the Be disc is coplanar with the orbital plane. The inner radius of the simulation region r_{in} is $3.0 \times 10^{-3} a$, where a is the semi-major axis of the binary. A polytropic equation of state with the exponent $\Gamma = 1.2$ is adopted. The Shakura-Sunyaev viscosity parameter $\alpha_{\text{SS}} = 0.1$ throughout the disc. There is also a bulk viscosity $\nu_b = 5\alpha_{\text{SS}}c_s H/3$, where c_s is the polytropic sound speed and H is the scale-height of the disc.

Fig. 1 gives a sequence of snapshots of the accretion disc around the neutron star for $7 \leq t \leq 8$ in model A, where the unit of time is the orbital period P_{orb} . The left panels show the contour maps of the surface density, whereas the non-axisymmetric components of the surface density and the velocity field are shown in the right panels. Annotated in each left panel are the time in units of P_{orb} , the relative disk thickness H/r at $r = 0.05a$ and the mode strength S_1 , a measure of the amplitude of the one-armed spiral wave, details of which will be described later. It is noted from the figure that the one-armed, trailing spiral is excited at periastron and is gradually damped towards the next periastron.

For comparison, we present the results for model B, in which the mass transfer is artificially turned off for $7 \leq t \leq 8$. Fig. 2 shows the surface density (the left panel) and the non-axisymmetric components of the surface density and the velocity field (the right panel) at the time corresponding to the middle panel of Fig. 1. The format of the figure is the same as that of Fig. 1. It should be noted that the disc deformation due to the one-armed mode is not seen in model B. The disc is more circular and has a larger radius in model B than in model A. This strongly suggests that the excitation of the one-armed spiral structure in the accretion disc is induced by ram pressure from the material transferred from the Be disc at periastron.

2.1 Mode strength

In this subsection, we analyse the orbital-phase dependence of the disc eccentricity by decomposing the surface den-

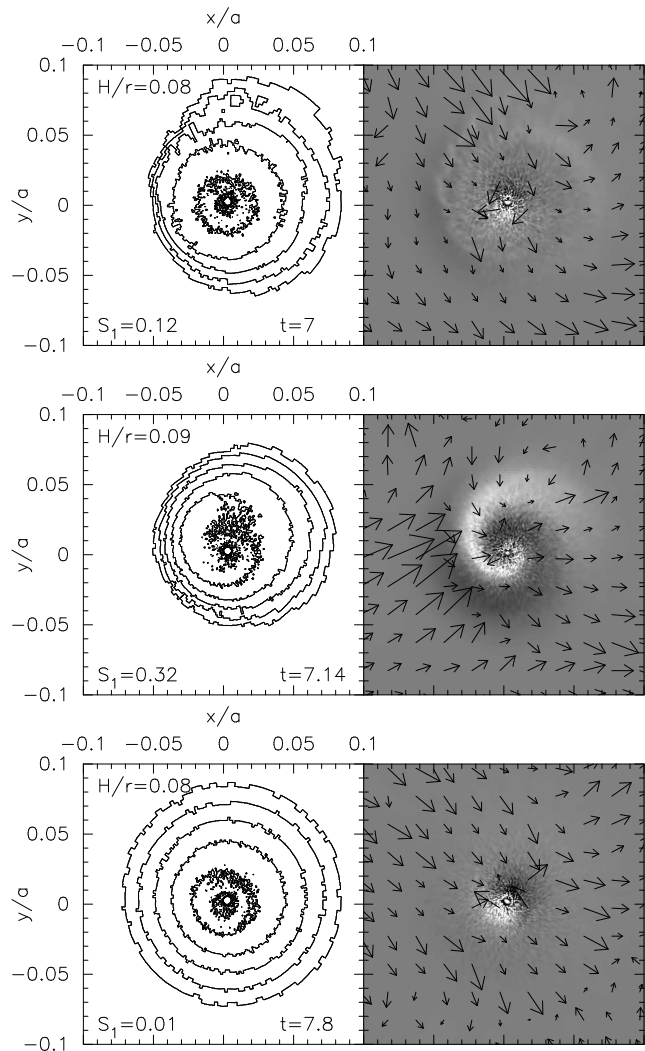


Figure 1. Snapshots of the accretion disc for model A. The left panels show the surface density in a range of three orders of magnitude in the logarithmic scale, while the right panels show the non-axisymmetric components of the surface density (gray-scale plot) and the velocity field (arrows) in the linear scale. In the right panels, the region in gray (white) denotes the region with positive (negative) density enhancement. The periastron is in the x -direction and the disc rotates counterclockwise. Annotated in each left panel are the time in units of P_{orb} , the relative disk thickness H/r at $r = 0.05a$ and the mode strength S_1 .

sity distribution into Fourier components which vary as $\exp(im\phi)$, where m is the azimuthal harmonic number.

Following Lubow (1991), we define the mode strength by

$$S_{f,m}(t) \equiv \frac{2}{M_d(1 + \delta_{m,0})} \int_r dr \int_0^{2\pi} r d\phi \Sigma(r, \phi, t) f(m\phi), \quad (1)$$

where f is either sin or cos and M_d is the total disc mass given by $\int_r dr \int_0^{2\pi} r d\phi \Sigma(r, \phi, t)$. Then, the total strength of the mode m is defined by

$$S_m(t) = (S_{\cos,m}^2 + S_{\sin,m}^2)^{1/2}. \quad (2)$$

Note that our definition of the mode strength slightly differs from that of Lubow (1991). He decomposed the surface density distribution into double Fourier components

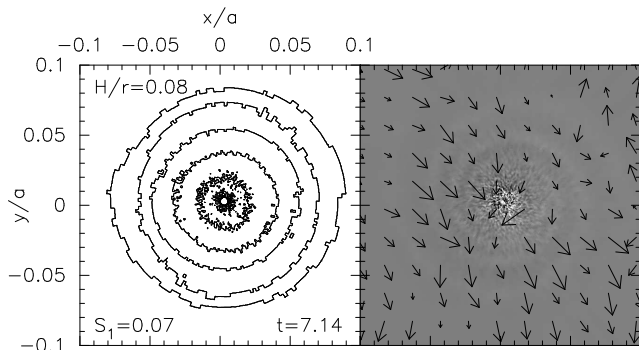


Figure 2. Same as Fig. 1, but for model B.

with the azimuthal and time harmonic numbers, whereas we did it with only the azimuthal harmonic number. This is because our purpose is to analyze the time dependence of the non-axisymmetric structure of the accretion disc in detail. Note also that the definition of the mode strength is not unique, so Eq. (2) gives only a rough measure of the amplitude of each mode. If the spiral wave is tightly winding, Eq. (2) will underestimate the amplitude significantly.

Fig. 3 shows the evolution of several non-axisymmetric modes for model A, in which the phase-dependent mass transfer from the Be disc is taken into account. The solid, dashed and dotted lines denote the strengths of $m = 1$, $m = 2$ and $m = 3$ modes, respectively. From Fig. 3, we note that the $m = 1$ component dominates the other components throughout the run. In the initial developing stage of the disc ($0 \leq t \leq 5$), elliptical orbits of the gas particles transferred from the Be disc significantly contribute to the strength of the $m = 1$ component, S_1 . The contribution becomes smaller as the disc develops. Thus, the decrease in S_1 for $t \lesssim 5$ corresponds to the decrease in the disc eccentricity during this period. The decrease in eccentricity is likely to result from a non-zero bulk viscosity which helps to prevent the spontaneous growth of the eccentricity through viscous overstability (Ogilvie 2001).

In contrast, after the disc is well developed ($t \gtrsim 5$), the one-armed spiral wave gives the major contribution to S_1 . The mode strength significantly modulates with orbital phase, corresponding to the rapid excitation and the subsequent gradual damping of the wave.

In order to see the time dependence of non-axisymmetric structure in the developed accretion disc more closely, we show the time dependence of the mode strength S_1 for $7 \leq t \leq 8$ in the top panel of Fig. 4. The thick and thin lines denote S_1 in model A and in model B, respectively. Recall that in model B the mass transfer from the Be disc is artificially turned off for this period.

In model A, the mode strength S_1 is dominated by the one-armed spiral mode. It rapidly increases to the maximum value of ~ 0.3 at $t = 7.14$ (see the middle panel of Fig. 1) and then gradually decreases to a minimum value of ~ 0.01 at $t = 7.8$ (the bottom panel of Fig. 1). It is important to note that the mode strength S_1 in model A is much stronger and has much larger orbital modulation than in model B. This clearly shows that the one-armed mode is not excited by the tidal interaction with the Be star but by ram pressure of the material transferred from the Be disc at periastron passage.

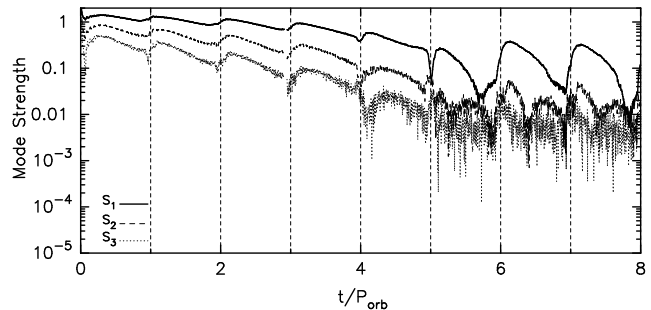


Figure 3. Evolution of several non-axisymmetric modes for $0 \leq t \leq 8$. The solid, dashed and dotted lines denote the strengths of the $m = 1$, $m = 2$ and $m = 3$ modes, respectively.

The middle panel of Fig. 4 shows the azimuth ω_p between the position vector of the maximum value of the non-axisymmetric component of the surface density and the eccentric vector of the binary orbit (hereafter, the azimuth of the maximum density perturbation). As in the other panels, the thick and thin lines are for model A and model B, respectively. It should be noted that ω_p in both models shifts little over one orbital period. This is a typical characteristic of the one-armed modes in nearly Keplerian discs (Kato 1983).

2.2 Orbital modulation in the disc radius

In paper I, we found that the disc size modulates with the orbital phase; the disc shrinks at periastron and gradually restores its radius afterwards. Our interpretation of this orbital modulation was that the decrease in the disc radius at periastron is due to a negative torque by the Be star, while the later expansion is due to the viscous diffusion. For the reason described below, this interpretation must be corrected.

The bottom panel of Fig. 4 shows the time dependence of the disc radius for $7 \leq t \leq 8$, which is defined in the same way as in paper I (equation 5). As in the other panels, the thick and thin lines are for model A and model B, respectively. From the figure, we note that the disc radius in model B monotonically increases with time and shows no orbital modulation. This is in sharp contrast to the orbital modulation in the disc radius seen in model A. Since the only difference between model A and model B is that the mass transfer from the Be disc is included in model A, while it is not in model B, it is most likely that the reduction in the disc radius after periastron passage is related to the mass transfer from the Be disc. Apparently, the negative torque by the Be star has little effect on the accretion disc radius in these models.

How can the mass transfer from the Be star reduce the accretion disc size? As shown in Fig. 3 of paper I, the circularization radius of the material transferred from the Be disc is smallest around the periastron. It is much smaller than the accretion disc radius shown in the bottom panel of Fig. 4. In other words, the specific angular momentum of the material transferred from the Be disc is much smaller than that of the material at the outer radius of the accretion disc. Accretion of such material onto the disc outer radius will temporarily reduce the disc radius. This mechanism, together with the

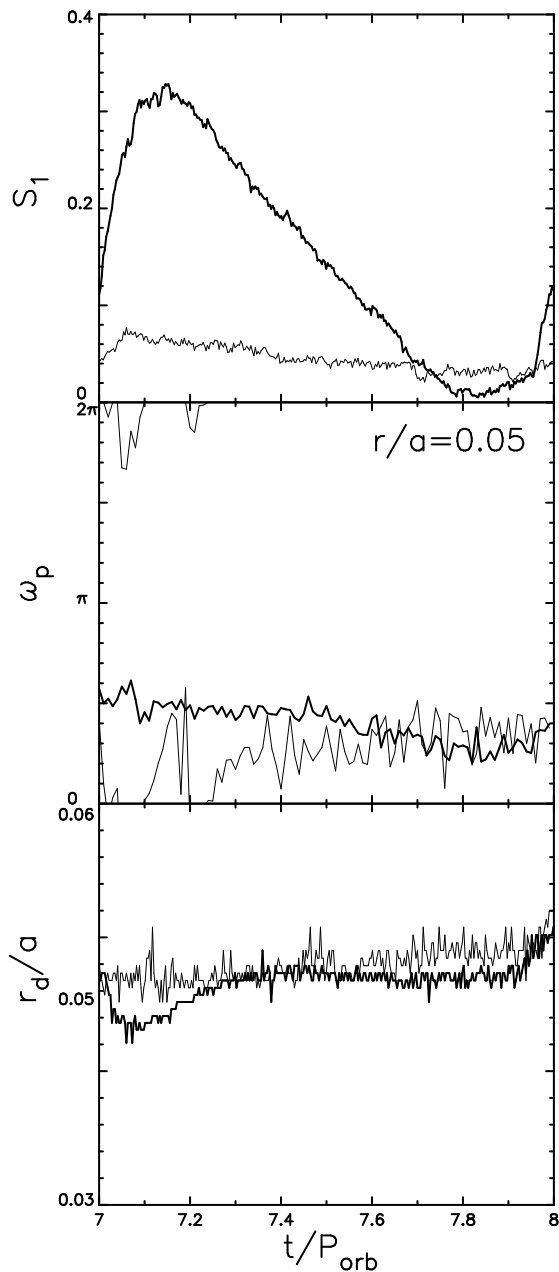


Figure 4. Time dependence of the mode strength S_1 , the azimuth of the maximum density perturbation, ω_p , at $r = 0.05a$, and the disc radius r_d for $7 \leq t \leq 8$. In each panel, the thick line is for model A, while the thin line for model B.

viscous diffusion, naturally explains the orbital modulation in the disc radius found in paper I.

2.3 Phase dependence of the accretion rate

After the accretion disc is developed ($t \gtrsim 5$), the mass-accretion rate has double peaks per orbit, a relatively-narrow, low peak at periastron and a broad, high peak afterwards [see Fig. 15(a) of paper I]. While the first low peak at periastron could be artificial, being related to the presence of the inner simulation boundary, the origin of the second high peak was not clear. Below we show that the one-armed

spiral wave is responsible for the second peak in the mass-accretion rate.

Fig. 5 shows the time dependence of the mass-accretion rate for $7 \leq t \leq 8$. The thick line denotes the mass-accretion rate in model A, in which the mass transfer from the Be disc is taken into account. For comparison, the mass-accretion rate in model B, in which the mass transfer from the Be disc is artificially turned off at $t = 7$, is also shown by the thin line. The difference between the accretion rate profiles for these two models is striking. The accretion rate in model B monotonically decreases over one orbital period, whereas that of model A shows a broad peak centred at $t \sim 7.32 - 7.35$, which corresponds to the second peak found in paper I.

Although it is obvious that the above peak is caused by the mass transfer from the Be disc, the mass transfer rate has a narrow peak at periastron. What mechanisms connecting the mass transfer from the Be disc and the mass accretion onto the neutron star lead to a phase delay of ~ 0.3 ? There are two possibilities. Either the disc is viscously adjusting to the addition of low-angular momentum material. However, even if the angular momentum of the material transferred from the Be disc is the lowest, its viscous time scale at the circularization radius is over 7 binary periods [see Fig. 3 of paper I]. Thus, the viscous accretion of the lowest-angular momentum material could play no key role of the enhancement of the accretion rate at an orbital phase of about 0.35. Or, the second possibility is that the one-armed spiral wave is excited by ram pressure of the transferred material from the Be disc and then the spiral wave travels inwardly. The excitation of the spiral wave takes about $\sim (0.1 - 0.2)P_{\text{orb}}$ (see the top panel of Fig. 4) and the difference of the peak position on the orbital phase between the mode strength and the accretion rate results from the wave propagation from the disc outer radius to the inner simulation boundary.

The time-scale for wave propagation is roughly estimated by using the dispersion relation of the one-armed oscillation in the nearly Keplerian discs (Kato 1983). Its frequency ω is written by $\omega \sim -\Omega_{\text{orb}}(k_r H)^2/2$, where k_r is the radial wavenumber and Ω_{orb} is the orbital angular velocity. Finally, the time-scale for a global, one-armed perturbation to travel across the disc is $2\pi/\omega \sim 0.13P_{\text{orb}}$ at $r \sim 0.05a$ at $t \sim 7.1$. Therefore, combining the time-scales for wave excitation and propagation, we expect that the peak of the mass-accretion rate lags behind that of the mass-transfer rate by $(0.2 - 0.3)P_{\text{orb}}$, which is in good agreement with the phase of the second peak of mass-accretion rate shown in Fig. 5.

3 CONCLUSIONS

In this *letter*, we have investigated non-axisymmetric structure in the accretion disc around the neutron star in Be/X-ray binaries, analysing the results from a simulation performed by Hayasaki & Okazaki (2004). We have adopted the phase-dependent, mass-transfer rate from a high-resolution simulation by Okazaki et al. (2002) for a coplanar system with a short period ($P_{\text{orb}} = 24.3$ d) and a moderate eccentricity ($e = 0.34$), which targeted 4U 0115+63, one of the best studied Be/X-ray binaries.

We have found that a one-armed, trailing spiral wave

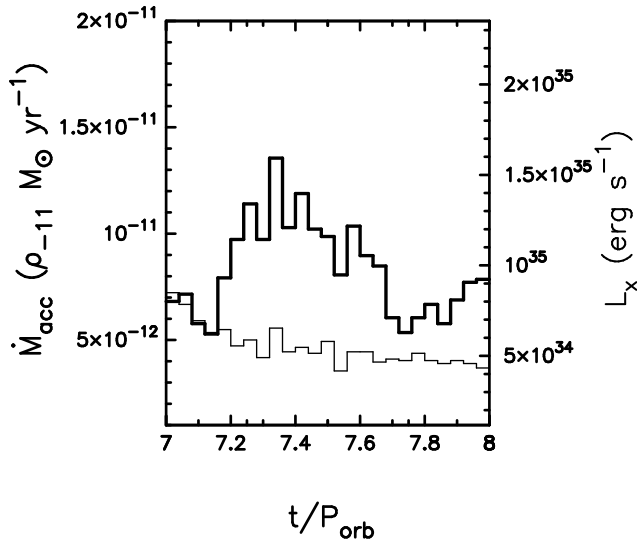


Figure 5. Time dependence of the mass-accretion rate for $7 \leq t \leq 8$. The thick and thin lines are for model A and model B, respectively. The right axis shows the X-ray luminosity corresponding to the mass-accretion rate.

is excited in the accretion disc by ram pressure from the strongly phase-dependent mass-transfer from the Be disc. The spiral wave is transient; it is excited at periastron passage, when mass transfer from the Be disc takes place, and is gradually damped afterwards. The one-armed perturbation pattern in the accretion disc precesses little over one orbital period, which is consistent with the theory of global, one-armed oscillations in nearly Keplerian discs (Kato 1983).

The eccentric ($m = 1$) mode dominates the other non-axisymmetric modes throughout the run ($0 \leq t \leq 8P_{\text{orb}}$). In the initial stage of disc development ($0 \leq t \leq 5P_{\text{orb}}$), elliptical orbits of the gas particles transferred from the Be disc make the accretion disc significantly eccentric. After the disc is well developed ($t \gtrsim 5$), however, the one-armed spiral wave gives the major contribution to the eccentric deformation of the accretion disc. Then, the strength of the deformation significantly modulates with the orbital phase, corresponding to the rapid excitation and the subsequent gradual damping of the one-armed wave.

The system we studied differs from that of Kato & Tosa (1994) in the sense that our accretion disc is nearly Keplerian and ram pressure of the material transferred from the Be disc exerts on the accretion disc only briefly around periastron. Nevertheless, we can estimate the growth rate of the one-armed spiral wave based on their formalism. According to Kato & Tosa (1994), the growth rate λ is given by $\lambda \simeq \pi v_r / (r_d - r_{\text{in}})$ where v_r is the radial velocity of the disc. In our case, adopting $v_r \sim 0.07a\Omega_{\text{orb}}$ at $r \sim r_d \sim 0.05a$, we have $\lambda \sim \Omega_K \gg \Omega_{\text{orb}}$ at $r = 0.05a$ for $7.0 \leq t \leq 7.2$. This explains the rapid growth of the spiral wave for $7.0 \leq t \leq 7.2$ in our simulation.

After the accretion disc has developed ($t \gtrsim 5P_{\text{orb}}$), the mass-accretion rate has double peaks per orbit, a relatively-narrow, low peak at periastron and a broad, high peak afterwards. We have found that the one-armed spiral wave excited by ram pressure of the material transferred from

the Be disc enhances the inward mass flux in the accretion disc, and is therefore responsible for this high peak in the accretion rate. The X-ray luminosity peak corresponding to the high peak in accretion rate has never been identified in Be/X-ray binaries. However, if this peak is detected, it could be understood as strong circumstantial evidence for the presence of an accretion disc in Be/X-ray binaries.

In this *letter*, we have reported on the effects of ram pressure on the accretion disc, including the excitation of the one-armed spiral wave, which enhances the accretion rate. These results are based on the simulations, of which the run time was much shorter than the viscous time-scale. In longer simulation runs, new features/interactions are expected to appear. While the deformation of the accretion disc by ram pressure is expected to become small as the disc mass increases, the excitation of the eccentric mode directly driven by the one-armed bar potential, which is not seen in our simulations, will become important. The tidal/resonant torque by the Be star may begin to work on the outer part of the accretion disc, as the disc size increases. In a subsequent paper, we will investigate the long-term evolution of the accretion disc in Be/X-ray binaries in detail.

ACKNOWLEDGEMENTS

We acknowledge the anonymous referee for constructive comments. KH thank James R. Murray for useful comments. The simulations reported here were performed using the facility at the Hokkaido University Information Initiative Center, Japan. This work has been supported by Grant-in-Aid for the 21st Century COE Scientific Research Programme on "Topological Science and Technology" from the Ministry of Education, Culture, Sport, Science and Technology of Japan (MECSST) and in part by Grant-in-Aid for Scientific Reserch (15204010 and 16540218) of Japan Society for the Promotion of Science.

REFERENCES

- Bate M.R., Bonnell I.A., Price N.M., 1995, MNRAS, 285, 33
- Benz W., 1990, in Buchler J. R., ed., The Numerical Modelling of Nonlinear Stellar Pulsations. Kluwer, Dordrecht, p.269
- Benz W., Bowers R.L., Cameron A.G.W., Press W.H., 1990, ApJ, 348, 647
- Hayasaki K & Okazaki A.T., 2004, MNRAS, 350, 971
- Hirose M & Osaki Y., 1989, PASJ, 42, 135
- Kato S., 1983, PASJ, 35, 249
- Kato S. & Tosa M., 1994, PASJ, 46, 559
- S H. Lubow., 1991, ApJ, 381, 268
- S H. Lubow., 1994, ApJ, 432, 224
- Okazaki A.T., Bate M.R., Ogilvie G.I & Pringle J.E., 2002, MNRAS, 337, 967
- Ogilvie G.I., 2001, MNRAS, 325, 231
- Tosa M., 1994, ApJL, 426, 81